ELSEVIER

Journal of Materials Processing Technology 97 (2000) 180–185

Journal of Materials Processing Technology

www.elsevier.com/locate/jmatprotec

A universal velocity field for the extrusion of non-axisymmetric rods with non-uniform velocity distribution in the extrusion direction

C.W. Wu, R.Q. Hsu*

Department of Mechanical Engineering, National Chiao Tung University, 1001 Ta-Hsueh Road, Hsinchu 300, Taiwan, ROC

Received 17 August 1998

Abstract

This study formulates a universal velocity field that is kinematically admissible for application in the extrusion of non-axisymmetric rods. Then upper bound theorem dictates that a better upper bound solution heavily depends on the precise conformity of the velocity field postulated. However, a compromise must frequently be made, since the formulation is in general rather complicated. The kinematically admissible velocity field proposed herein has the following features: (a) it is three-dimensional, (b) it is non-uniformally distributed in the axial direction, and (c) the formulation is straight-forward once the boundary of the deformation zone is specified. In addition, the velocity field is applied to the extrusion of rectangular, hexagonal, and octagonal rods from round billets. Moreover, the extrusion loads are calculated against process variables such as the semi-die angle, the percentage reduction of area, and the friction factor. Furthermore, the velocity field is compared with results from the literature, indicating that the present results render a better upper bound solution for application in extrusion than do previous results. © 2000 Published by Elsevier Science S.A. All rights reserved.

Nomenclature

r, ϕ, y	cylindrical coordinates
R_0, $R_f(\phi)$	radius of the billet before extrusion and the product profile function after extrusion, respectively
$Rs_0(\phi,y)$	a function that represents the die surface
V_0, V_f	entrance velocity of the billet and exit velocity of the extruded product, respectively
Γ_s, Γ_f	surfaces of shear velocity discontinuities and friction, respectively
V_r, V_ϕ, V_y	velocity components of the billet in cylindrical coordinates (r,ϕ,y), respectively
$\omega(\phi,y)$	angular velocity of the billet
$U(y)$, $D(r,\phi,y)$	uniform and non-uniform velocity component along the extrusion axis of the billet, respectively
$\partial U(r)/\partial y$	first derivative of the uniform velocity component along the extrusion axis of the billet with respect to y
$\partial\omega(\phi,y)/\partial y$	first derivative of the angular velocity of the billet with respect to ϕ
$Z(\phi,y)$	function of (β,Rs_0,L)
$\partial Z(\phi,y)/\partial y$	first derivative of function $Z(\phi,y)$ with respect to y
$\partial Rs_0(\phi,y)/\partial y$	first derivative of the die surface function with respect to y
$\partial Rs_0(\phi,y)/\partial\phi$	first derivative of the die surface function with respect to ϕ
$\phi_f(y)$	angle of a surface of geometrical symmetry
β	optimization parameter introduced in the velocity field
L	die length(dimensionless)
J	total power consumption in extrusion
$\dot{W}_i$, $\dot{W}_s$, $\dot{W}_f$	power dissipation due to internal deformation, internal shear of the billet and friction at the die surface, respectively
V_p	volume of the plastic region
σ_y, $\dot{\bar{\varepsilon}}$	the yield stress and effective strain rate of the material, respectively
$\dot{\varepsilon}_{ij}$	components of the strain rate tensor
$\Delta V_{\Gamma_s}, \Delta V_{\Gamma_f}$	the relative slip velocity on $\Gamma_s$and Γ_f surfaces, respectively

*Corrresponding author. Tel.: 886-3-5731934; fax: 886-3-5738061
E-mail address: u8114539@cc.nctu.edu.tw (R.Q. Hsu)

0924-0136/00/$ – see front matter © 2000 Published by Elsevier Science S.A. All rights reserved.
PII: S0924-0136(99)00364-7

P_{avg}	average extrusion pressure
α	semi-die angle
R.A.	reduction of the area of the billet
m	friction factor at the die surface

1. Introduction

Non-axisymmetric extrusion, which is used widely to produce rectangular, hexagonal and other non-regular sections, has received increasing interest. Hill [1] demonstrated the feasibility of three-dimensional analysis of the metal-working process. Juneja and Prakash [2] derived an upper bound solution to extrude rod with a polygonal cross-section through straightly converging dies, by utilizing a spherical velocity field with a cylindrical surface of velocity discontinuity. In a related investigation, Boer and Webster [3] obtained an upper bound solution to draw square sections from a round billet. Later, Hoshino and Gunasekera [4–7] proposed an upper bound model to extrude polygonal sections from a round billet. Yang and Lee [8] proposed the conformal mapping approach to derive a kinematically admissible velocity field for extrusion through concave and convex shaped dies. Yang et al. [9] also analyzed the three-dimensional extrusion of arbitrarily-shaped sections. Kiuchi et al. [10,11] derived a three-dimensional velocity field for non-symmetric extrusion. However, owing to the complexity of establishing the three-dimensional kinematically admissible velocity field, the above investigations assumed that the velocity component in the extrusion direction is uniform at any cross-section. However, such an assumption does not conform to the actual deformation behavior.

In this study, the authors present a novel numerical model based on the upper bound theorem to analyze the extrusion of non-axisymmetric rods with an arbitrary section profile (Fig. 1). This model is advantageous in that the three-dimensional kinematically admissible velocity field has a non-uniform velocity component in the extrusion direction. In addition, establishing the velocity field is relatively simple and straight-forward once the die profile function is known. The derived velocity field is applied to the extrusion of rectangular, hexagonal, octagonal and round rods to demonstrate the effectiveness of the proposed method. Finally, comparison of the present results with available results from the literature reveals a close correspondence.

2. Derivation of the velocity field

When applying the upper bound approach to analyze plastic deformation, a properly constructed admissible velocity field is deemed essential to ensure the accuracy of the final solution. To be admissible, the velocity components must fulfill the conditions of incompressibility, and the

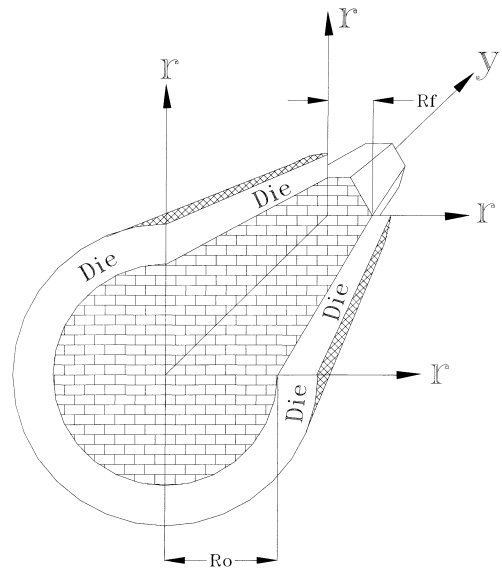

Fig. 1. Schematic diagram of the extrusion of a hexagonal shaped section rod.

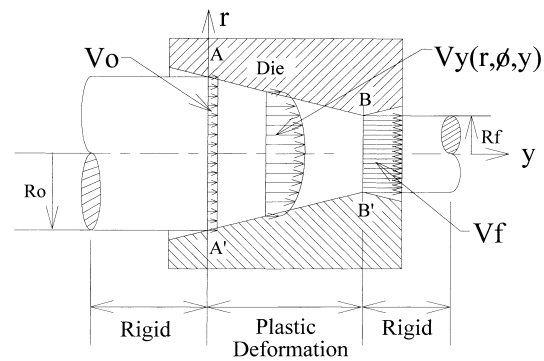

Fig. 2. Velocity component along the y-axis.

boundary conditions required by the geometry, and must be continuous except at particular surfaces where velocity slips are allowed. Thus, the geometrical configuration of the material during plastic deformation must be known. In the extrusion process, the geometrical configuration of the billet is confined by the die surface. If function $Rs_0(\phi,y)$ represents the billet geometry in the deformation zone, then, according to condition of incompressibility:

$$\int_0^{\phi_f 0}\int_0^{R_0} V_0 r\,dr\,d\phi = \int_0^{\phi_f y}\int_0^{Rs_0\phi,y} V_y(r,\phi,y)r\,dr\,d\phi, \qquad (1)$$

where (as shown in Fig. 2) V_0 denotes the velocity of the billet before entering the die entrance plane A–A′, and $V_y(r,\phi,y)$ represents the velocity component of billet in the extrusion direction during plastic deformation, i.e. the section bounded by the die surface, die entrance plane and the die exit plane B–B′. When the material leaves the die exit plane, it moves forward under a uniform speed V_f. If R_0 is the radius of the billet before extrusion, then $Rs_0(\phi,y)$ is a function representing the geometrical configuration of the

billet during deformation. In addition, $\phi_f(0)$ and $\phi_f(y)$ are the ranges of integration in the ϕ direction at $y=0$ and $y=y$, respectively. To accommodate a non-uniform component of velocity along the extrusion axis, a convex distribution function $D(r,\phi,y)$ is introduced herein, i.e.:

$$V_y(r,\phi,y) = D(r,\phi,y)U(y) = \left[1-\frac{4\beta y(L-y)}{Rs_0^2(\phi,y)L^2}r^2\right]U(y), \tag{2}$$

where $U(y)$ is the uniform component of $V_y(r,\phi,y)$ The convexity of $V_y(r,\phi,y)$ is determined by the parameter β, which is subjected to optimization when calculating the total energy. L denotes the length of deformation zone. $V_y(r,\phi,y)$ is also subjected to the following boundary conditions:

$$V_y(r,\phi,0) = U(0), \quad V_y(r,\phi,L) = U(L). \tag{3}$$

Substituting Eq. (2) into Eq. (1) and rearranging yields:

$$U(y) = \frac{V_0\int_0^{\phi_f 0} Rs_0^2(\phi,0)\mathrm{d}\phi}{\left(1-\frac{2\beta y(L-y)}{L^2}\right)\int_0^{\phi_f y} Rs_0^2(\phi,y)\mathrm{d}\phi}. \tag{4}$$

The condition of incompressibility can be expressed as:

$$\dot{\varepsilon}_{rr}+\dot{\varepsilon}_{\phi\phi}+\dot{\varepsilon}_{yy} = \frac{\partial V_r(r,\phi,y)}{\partial r} + \frac{1}{r}\left[V_r(r,\phi,y)+\frac{\partial V_\phi(r,\phi,y)}{\partial\phi}\right]+\frac{\partial V_y(r,\phi,y)}{\partial y} = 0. \tag{5}$$

To simplify the formulation of the velocity field, the rotational velocity component is assumed to be distributed linearly over the radius, i.e.:

$$V_\phi(r,\phi,y) = r\cdot w(\phi,y). \tag{6}$$

At the axis of extrusion, $r=0$, the velocity component $V_y(r,\phi,y)$ must be zero. Substituting Eqs. (2) and (6) into Eq. (5) and rearranging leads to:

$$V_r(r,\phi,y) = -\frac{r}{2}\left[\frac{\partial U(y)}{\partial y}+\frac{\partial w(\phi,y)}{\partial\phi}\right] + \frac{r^3}{4}\left[Z(\phi,y)\frac{\partial U(y)}{\partial y}+\frac{\partial Z(\phi,y)}{\partial y}U(y)\right]. \tag{7}$$

Here,

$$Z(\phi,y) = \frac{4\beta y(L-y)}{Rs_0^2(\phi,y)L^2}. \tag{8}$$

On the other hand, at $r = Rs_0(\phi,y)$, the material must flow along the die surface. Thus:

$$\begin{aligned} V_r(Rs_0(\phi,y),\phi,y) &= V_\phi(Rs_0(\phi,y),\phi,y)\frac{1}{Rs_0(\phi,y)}\frac{\partial Rs_0(\phi,y)}{\partial\phi} + V_y(Rs_0(\phi,y),\phi,y)\frac{\partial Rs_0(\phi,y)}{\partial y} \\ &= w(\phi,y)\frac{\partial Rs_0(\phi,y)}{\partial\phi} + V_y(Rs_0(\phi,y),\phi,y)\frac{\partial Rs_0(\phi,y)}{\partial y}. \end{aligned} \tag{9}$$

At the angle of symmetry surface $\phi_f(y)$, there exist no rotational velocity, thereby leading to $\omega(\phi_f(y),y)=0$. Combining Eqs. (7) and (9), rearranging leads to:

$$\omega(\phi,y) = -\frac{2}{Rs_0^2(\phi,y)}\int_0^{\phi_f y}\left\{V_y(Rs_0(\phi,y),\phi,y)Rs_0(\phi,y)\times\frac{\partial Rs_0(\phi,y)}{\partial y}+\frac{Rs_0^2(\phi,y)}{2}\frac{\partial U(y)}{\partial y}-\frac{Rs_0^4(\phi,y)}{4}\times\left[\frac{\partial Z(\phi,y)}{\partial y}U(y)+Z(\phi,y)\frac{\partial U(y)}{\partial y}\right]\right\}\mathrm{d}\phi. \tag{10}$$

The velocity components becomes:

$$V_y(r,\phi,y) = D(r,\phi,y)U(y) = \left[1-\frac{4\beta y(L-y)}{Rs_0^2(\phi,y)L^2}r^2\right]U(y), \tag{11}$$

$$V_\phi(r,\phi,y) = r\cdot\omega(\phi,y), \tag{12}$$

$$V_r(r,\phi,y) = -\frac{r}{2}\left[\frac{\partial U(y)}{\partial y}+\frac{\partial\omega(\phi,y)}{\partial\phi}\right] + \frac{r^3}{4}\left[Z(\phi,y)\frac{\partial U(y)}{\partial y}+\frac{\partial Z(\phi,y)}{\partial y}U(y)\right]. \tag{13}$$

Here,

$$U(y) = \frac{V_0\int_0^{\phi_f 0} Rs_0^2(\phi,0)\mathrm{d}\phi}{\left(1-\frac{2\beta y(L-y)}{L^2}\right)\int_0^{\phi_f y} Rs_0^2(\phi,y)\mathrm{d}\phi}, \tag{14}$$

$$\omega(\phi,y) = -\frac{2}{Rs_0^2(\phi,y)}\int_0^{\phi_f y}\left\{V_y(Rs_0(\phi,y),\phi,y)Rs_0(\phi,y)\times\frac{\partial Rs_0(\phi,y)}{\partial y}+\frac{Rs_0^2(\phi,y)}{2}\frac{\partial U(y)}{\partial y}-\frac{Rs_0^4(\phi,y)}{4}\times\left[\frac{\partial Z(\phi,y)}{\partial y}U(y)+Z(\phi,y)\frac{\partial U(y)}{\partial y}\right]\right\}\mathrm{d}\phi, \tag{15}$$

$$Z(\phi,y) = \frac{4\beta y(L-y)}{Rs_0^2(\phi,y)L^2}. \tag{16}$$

One of the characteristics of this velocity field state is that when function $Rs_0(\phi,y)$ is known, all of the velocity components can be readily formulated. According to the velocity field formulated above, the strain rate can be calculated as follows:

$$\dot{\varepsilon}_{rr} = \frac{\partial V_r(r,\phi,y)}{\partial r}, \quad \dot{\varepsilon}_{\phi\phi} = \frac{1}{r}\frac{\partial V_\phi(r,\phi,y)}{\partial\phi}+\frac{V_r(r,\phi,y)}{r}, \quad \dot{\varepsilon}_{yy} = \frac{\partial V_y(r,\phi,y)}{\partial y}, \tag{17}$$

$$\dot{\varepsilon}_{r\phi} = \frac{1}{2}\left[\frac{\partial V_\phi(r,\phi,y)}{\partial r}-\frac{V_\phi(r,\phi,y)}{r}+\frac{1}{r}\frac{\partial V_r(r,\phi,y)}{\partial\phi}\right],$$

$$\dot{\varepsilon}_{\phi y} = \frac{1}{2}\left[\frac{\partial V_\phi(r,\phi,y)}{\partial y}+\frac{1}{r}\frac{\partial V_y(r,\phi,y)}{\partial\phi}\right],$$

$$\dot{\varepsilon}_{yr} = \frac{1}{2}\left[\frac{\partial V_r(r,\phi,y)}{\partial y}+\frac{\partial V_y(r,\phi,y)}{\partial r}\right].$$

3. Upper bound solution

The upper bound theorem specifies that the power, J, consumed in the plastic deformation zone should be minimized with respect to β for the actual velocity field:

$$J = \dot{W}_i + \dot{W}_s + \dot{W}_f. \tag{18}$$

The internal deformation power, $\dot{W}_i$, is:

$$\dot{W}_i = \int_{V_p} \sigma_y \cdot \dot{\bar{\varepsilon}} \mathrm{d}V = \frac{2}{\sqrt{3}} \int_0^L \int_0^{\phi_f y} \int_0^{Rs_0\phi,y} \sigma_y \cdot \left(\frac{1}{2}\dot{\varepsilon}_{ij}\dot{\varepsilon}_{ij}\right)^{1/2} r\mathrm{d}r\mathrm{d}\phi\mathrm{d}y. \tag{19}$$

The shear power $\dot{W}_s$ is attributed to the velocity discontinuity (slip) on the rigid-plastic zone interface, plane A–A′ and B–B′; i.e.:

$$\dot{W}_s = \int_{\Gamma_s} \frac{1}{\sqrt{3}} \cdot \sigma_y \cdot \Delta V_{\Gamma_s} \mathrm{d}s = \frac{1}{\sqrt{3}} \int_0^{\phi_f 0} \int_0^{Rs_0\phi,0} \sigma_y \cdot \left[V_\phi^2(r,\phi,0) + V_r^2(r,\phi,0)\right]^{1/2} r\mathrm{d}r\mathrm{d}\phi + \frac{1}{\sqrt{3}} \int_0^{\phi_f L} \int_0^{Rs_0\phi,L} \sigma_y \cdot \left[V_\phi^2(r,\phi,L) + V_r^2(r,\phi,L)\right]^{1/2} r\mathrm{d}r\mathrm{d}\phi. \tag{20}$$

In this study, the friction factor m is used to calculate the friction energy loss on the die surface and m is deemed constant during the extrusion process. Thus, the friction power dissipated on die surface, $\dot{W}_f$, becomes:

$$\dot{W}_f = \int_{\Gamma_f} \frac{m}{\sqrt{3}} \cdot \sigma_y \cdot \Delta V_{\Gamma_f} \mathrm{d}s = \frac{m}{\sqrt{3}} \int_0^L \int_0^{\phi_f y} \sigma_y \cdot \Delta V_{\Gamma_f} \cdot \left\{1 + \left[\frac{\partial Rs_0(\phi,y)}{\partial y}\right]^2 + \left[\frac{1}{Rs_0(\phi,y)} \frac{\partial Rs_0(\phi,y)}{\partial \phi}\right]^2\right\}^{1/2} Rs_0(\phi,y)\mathrm{d}\phi\mathrm{d}y, \tag{21}$$

where:

$$\Delta V_{\Gamma_f} = \left\{V_r^2(r,\phi,y) + V_\phi^2(r,\phi,y) + V_y^2(r,\phi,y)\right\}^{1/2}. \tag{22}$$

4. Results and discussion

To demonstrate the effectiveness of the proposed velocity field, several non-axisymmetric extrusions are selected as the objects of study, i.e. from round rod to square, hexagonal and octagonal sections. The dies used herein are equal-angle divided and linearly connected converging dies as shown in Fig. 3. In this manner, $Rs_0(\phi,y)$ can be expressed as:

$$Rs_0(\phi,y) = \left\{R_0 - \left[(R_0 - R_f(\phi)) \cdot \frac{y}{L}\right]\right\}, \tag{23}$$

where $R_f(\phi)$ is the exit profile function of the billet. Owing to the entrance and exit cross-sections not being of the same shape, the semi-die angle in this study is defined as half of the die surface inclination in all of the calculations that follow. The results are shown below.

Fig. 4 indicates that for extrusion at small semi-die angles, the pressures required are larger than those for larger semi-die angles. Increasing the semi-die angle implies a gradual decrease of extrusion pressure, which then reaches a minimum pressure. Beyond this optimal semi-die angle, the extrusion pressure increases with the semi-die angle. Such an increase is due to that the two dominant components of

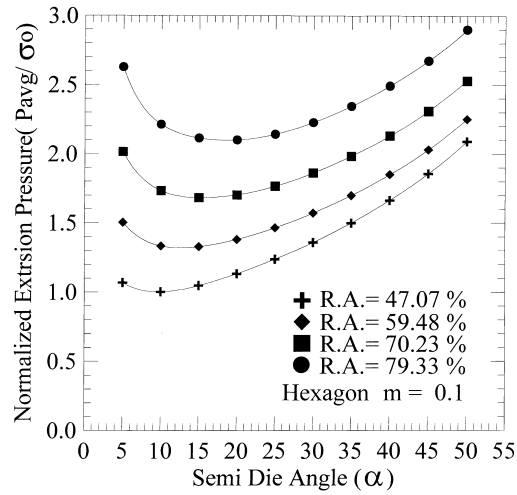

Fig. 4. Effects of the semi-die angle on the extrusion pressure.

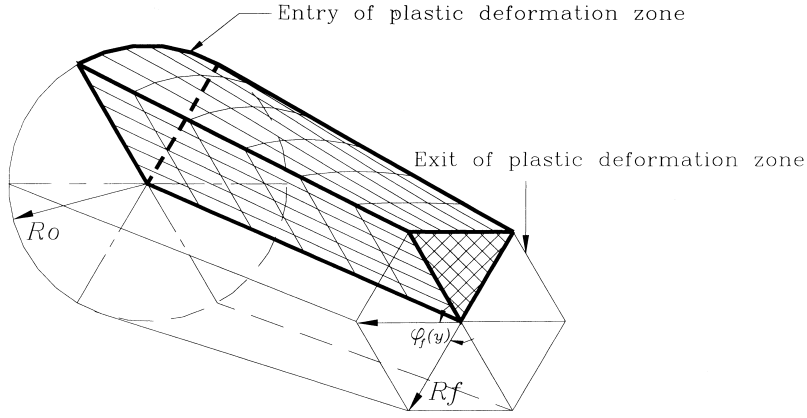

Fig. 3. Extrusion die for a hexagonal cross-section.

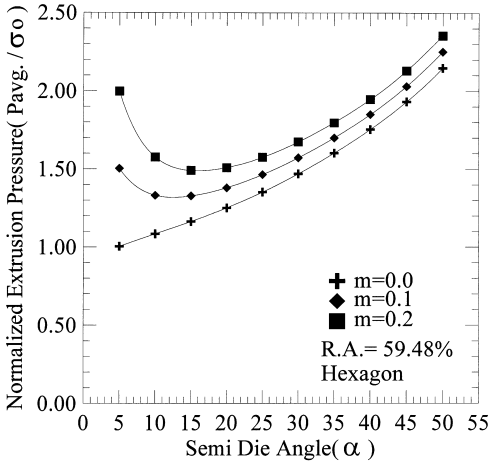

Fig. 5. Effects of the friction factor m on the extrusion pressure.

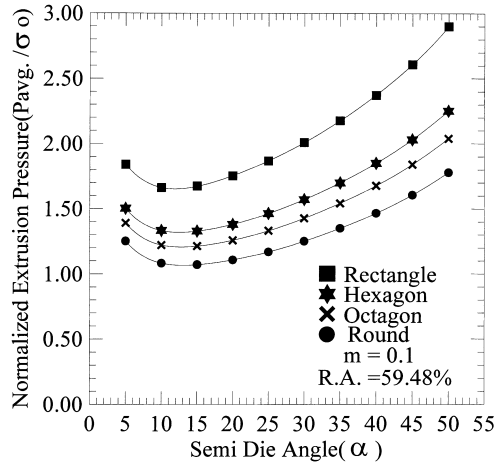

Fig. 7. Effects of the product shape on the extrusion pressure.

the power consumed in the extrusion process, i.e., the internal deformation power and the friction power conflict with each other. With a smaller semi-die angle, the length of contact between the billet and the die is longer, causing significantly high friction losses. On the other hand, for a larger semi-die angle, the die length is shorter; thus, the internal deformation becomes a predominant factor. According to Fig. 4, the extrusion pressure increases with an increase of the reduction of area at the same semi-die angle. For the working conditions indicated in the figure, the extrusion pressures apparently reach a minimum at a semi-die angle of between 10° and 20°.

Fig. 5 illustrates the effects of friction factor m on the extrusion pressure. Herein, the extrusion pressure increases with an increasing friction factor. If the friction factor m is zero, no power losses occur on the die surface. The total extrusion pressure consists mainly of the internal deformation component. Fig. 6 displays the parameter β against friction factor m. Eq. (2) clearly indicates that when β is large, the $V_y(r,\phi,y)$ at die surface is small. This finding suggests that the distribution of $V_y(r,\phi,y)$ over the radius has a more prominent convexity. For a larger friction factor m, the die surfaces are more sticky; the velocity component along the extrusion axis tends to be distorted more severely also. Therefore, β increases with an increase of friction factor m.

Fig. 7 presents the influence of the product shape by plotting the extrusion pressure against the number of section sides. According to this figure, the extrusion pressure is larger when the number of sides of the exit cross-section is smaller. Although the difference between two product shapes in terms of the extrusion pressure is appreciable, it decreases with an increase of the number of section sides. When the number of section sides increases, the product cross-section approaches circular and the extrusion pressure is closer to that of axisymmetric extrusion.

An important features in this study is that the velocity component in the extrusion axis is not uniform. Fig. 8 summarizes the effects of β on the extrusion pressure. This figure reveals that for the given set of process variables, the extrusion pressure calculated with a uniform velocity along the extrusion axis exceeds that of the non-uniform velocity field. On the other hand, the larger the semi-die angle implies a more severe deformation. Thus, the effect of β

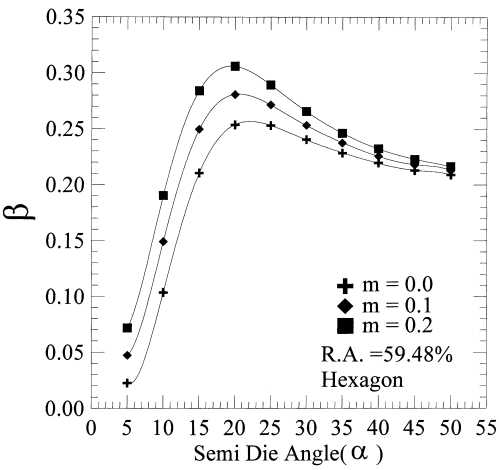

Fig. 6. Effects of the friction factor m on β.

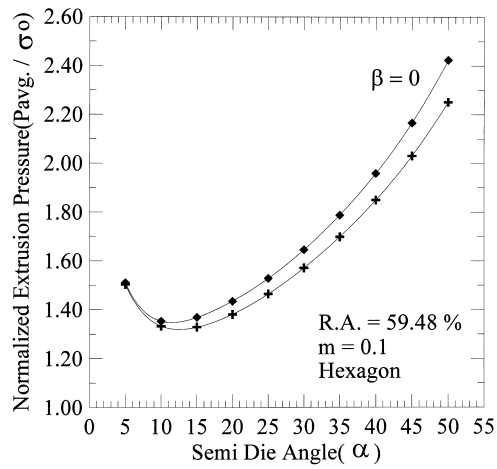

Fig. 8. Effects of β on the extrusion pressure.

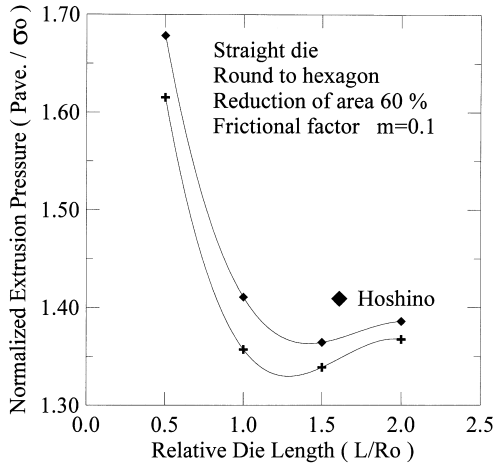

Fig. 9. Comparison of the present result with those of Hoshino [7] for the extrusion pressure.

is more prominent, as indicated from the difference in the extrusion pressure.

Fig. 9 compares the results of this study with the upper bound solution of Gunasekera and Hoshino [7]. According to this figure, extrusion pressures are shown against the relative die length (L/R_0). These comparisons reveal that the proposed method offers a superior upper bound solution.

5. Conclusions

This study present a novel model based on the upper bound theorem and, then, applies it to the extrusion of non-axisymmetric-shaped sections. The kinematically admissible velocity field formulated has a convex velocity distribution along the extrusion axis. The model proposed herein is applied to the extrusion of rectangular, hexagonal, and octagonal sections. The extrusion pressures are plotted against various variables such as semi-die angle, friction factor and reduction ratio. Based on the results in this study, the following can be concluded.

1. The extrusion pressure is the lowest for semi-die angle of between 10° and 20°.
2. A higher friction factor renders more severe velocity distortions in the extrusion direction for a given die geometrical configuration.
3. Shape complexity significantly influences the extrusion pressure. For the same round billet, the extrusion pressure decreases with an increase of the number of sides of the section of the product.
4. The proposed three-dimensional velocity field renders a better upper bound solution than the existing mode [7]. It can also be applied to extrude sections with arbitrary cross-sectional shapes.

References

[1] R. Hill, A general method of analysis for metal-working process, J. Mech. Phy. Solids 11 (1963) 305–326.
[2] B.L. Juneja, R. Prakash, An analysis for drawing and extrusion of polygonal section, Int. J. Mach Tool Des. Res. 15 (1975) 1–30.
[3] C.R. Boer, W.D. Webster, Direct upper-bound solution and finite element approach to round-to square drawing, J. Eng. Ind. 107 (1985) 254–260.
[4] S. Hoshino, J.S. Gunasekera, An upper-bound solution for the extrusion of square section from round bar through converging dies, Proceedings of 21st International Machine Tool Design Research Conference, Swansea, 1980, pp. 97–105.
[5] J.S. Gunasekera, S. Hoshino, Extrusion of noncircular sections through shaped dies, Annals of CIPP 29(1) (1980) 141–145.
[6] J.S. Gunasekera, S. Hoshino, Analysis of extrusion or drawing of polygonal sections through straightly converging dies, J. Eng. Ind. 104 (1982) 38–45.
[7] J.S. Gunasekera, S. Hoshino, Analysis of extrusion of polygonal sections through streamlined dies, J. Eng. Ind. 107 (1985) 229–233.
[8] D.Y. Yang, C.H. Lee, Analysis of three-dimension extrusion of sections through curved dies by conformal transformation, Int. J. Mech. Sci. 20 (1978) 541–552.
[9] D.Y. Yang, C.H. Han, M.U. Kim, A generalized method for analysis of three-dimensional extrusion of arbitrarily-shaped sections, Int. J. Mech. Sci. 28(8) (1986) 517–534.
[10] M. Kiuchi, H. Kishi, M. Ishikawa, Upper bound analysis of extrusion and/or drawing of square, rectangular, hexagonal and other asymmetric bars and wires — study on non-symmetric extrusion and drawing I, J. JSTP 24(266) (1983) 290–296.
[11] M. Kiuchi, M. Ishikawa, Upper bound analysis of extrusion and/or drawing of L-, T-, and H- sections — study on non-symmetric extrusion and drawing II, J. JSTP 24(270) (1983) 722–729.